

# RSC Advances



This is an *Accepted Manuscript*, which has been through the Royal Society of Chemistry peer review process and has been accepted for publication.

*Accepted Manuscripts* are published online shortly after acceptance, before technical editing, formatting and proof reading. Using this free service, authors can make their results available to the community, in citable form, before we publish the edited article. This *Accepted Manuscript* will be replaced by the edited, formatted and paginated article as soon as this is available.

You can find more information about *Accepted Manuscripts* in the [Information for Authors](#).

Please note that technical editing may introduce minor changes to the text and/or graphics, which may alter content. The journal's standard [Terms & Conditions](#) and the [Ethical guidelines](#) still apply. In no event shall the Royal Society of Chemistry be held responsible for any errors or omissions in this *Accepted Manuscript* or any consequences arising from the use of any information it contains.

## Annealing-Free Anatase TiO<sub>2</sub> Nanocrystal Film as Electron Collection Layer in Organic Solar Cells

Di Li,<sup>a</sup> Yanli Chen,<sup>b</sup> Peng Du,<sup>a,b</sup> Zhao Zhao,<sup>a</sup> Haifeng Zhao,<sup>a</sup> Yuejia Ma,<sup>a</sup> and Zaicheng Sun<sup>\*a</sup>

Received 00th January 20xx,  
Accepted 00th January 20xx

DOI: 10.1039/x0xx00000x

www.rsc.org/

Anatase TiO<sub>2</sub> film, which is traditionally fabricated by high-temperature annealing of TiO<sub>x</sub> precursors, has been widely used as electron collection layer in photovoltaics. In order to avoid the undesired high temperature treatment, in this work, we developed a convenient and moderate procedure to fabricate anatase TiO<sub>2</sub> nanocrystal film at room temperature. Ultrafine, clean and high-quality anatase TiO<sub>2</sub> nanocrystals have been pre-prepared in a simple solvothermal route and subsequently spin-coating the nanocrystal dispersion provides a well performed TiO<sub>2</sub> nanocrystal film without any further thermal treatment. The characteristics of TiO<sub>2</sub> nanocrystal film, in terms of crystallization phase, film morphology, optical and electronic properties, have been carefully studied, and at last, a typical [ITO/TiO<sub>2</sub>/P3HT:PCBM/MoO<sub>3</sub>/Ag] inverted photovoltaic device using TiO<sub>2</sub> nanocrystals as ECL has been fabricated and exhibits comparable power conversion efficiency (PCE) of 3.35% to that of the conventional device (3.39% PCE).

### Introduction

Organic solar cells (OSCs) have attracted much attention in recent years because of their appealing advantages of low cost, light weight and mechanical flexibility comparing with conventional silicon solar cells.<sup>1–5</sup> In order to improve the performances and stabilities of OSCs, besides elegantly optimizing the material systems and nanoscale phase separations, effectively collecting the charge carriers should also be focused on.<sup>6–8</sup> Indeed, electron collection layers play a crucial role in influencing the device performance for their energy-aligning capabilities, and of the reported ECLs, anatase TiO<sub>2</sub> is much attractive for its high environmental stability, suitable energy levels and high electron mobility.<sup>9–15</sup>

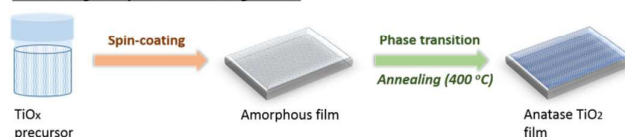
The most common approach to fabricate anatase TiO<sub>2</sub> ECL is high-temperature annealing (above 400 °C) to thoroughly transform amorphous TiO<sub>x</sub> precursors into anatase TiO<sub>2</sub> (scheme 1).<sup>9, 16</sup> Apparently, the annealing process complicates the device fabrication and limits the applications in thermal sensitive substrates. In order to overcome this defect, several approaches have been developed to construct TiO<sub>2</sub> ECLs in mild conditions, such as atomic layer deposition, electrochemical deposition, electrospray, high-pressure crystallization, chemical vapor deposition, chemical sintering and nanocomposites.<sup>17–22</sup> However, these methods require

either strict experimental conditions or complex TiO<sub>x</sub> sol-gel precursors, thus restrain the availability and simplicity of device processing. Therefore, it remains a great challenge for exploring a highly efficient and convenient approach to fabricate high-quality anatase TiO<sub>2</sub> film as ECL in thin film photovoltaics at low temperature.

#### This method



#### Common high-temperature annealing method



**Scheme 1.** Illustration of the approach in this work and common high-temperature annealing method to fabricate anatase TiO<sub>2</sub> film as ECL for photovoltaics.

For common high-temperature annealing method, the essential phase transition to obtain anatase TiO<sub>2</sub> film was achieved above 400 °C and herein, we envisioned that the pre-prepared anatase TiO<sub>2</sub> followed by filming could avoid the undesired high temperature treatment (scheme 1). Recently it has been reported that the nanocrystal layer of ultrafine n-type semiconductor ZnO could serve as effective electron collection layer in perovskite solar cells<sup>23</sup>. Moreover, Snaith's group<sup>24</sup> and Boyen's group<sup>25</sup> separately reported similar approaches to fabricated nanocrystal TiO<sub>2</sub> films as ECLs. However, due to the large size of TiO<sub>2</sub> nanoparticles (diameter of around 4.5 nm and 6 nm, respectively), the addition of

<sup>a</sup> State Key Laboratory of Luminescence and Applications, Fine Mechanics and Physics, Chinese Academy of Sciences, 3888 East Nanhu Road, Changchun, Jilin 130033, P. R. China. E-mail: [sunzc@ciomp.ac.cn](mailto:sunzc@ciomp.ac.cn)

<sup>b</sup> Institute for New Energy Materials & Low-Carbon Technologies, School of Materials Science and Engineering, Tianjin University of Technology, Tianjin 300384, P. R. China.

† Electronic Supplementary Information (ESI) available: Additional figures of HRTEM, AFM, UPS, SCLC and UV-Vis absorption. See DOI: 10.1039/x0xx00000x

TiAcAc served as “electronic glue” and annealing at 135–150 °C to decompose TiAcAc to  $\text{TiO}_x$  and remove organic impurities were essential to fill the gaps between the large nanoparticles. In this work, we developed a convenient and moderate procedure to synthesize ultrafine (with diameter around 2–3 nm) and high-quality anatase  $\text{TiO}_2$  nanocrystals without any additional surfactants or binders; then simply spin-coat the nanocrystal dispersion to give high-quality anatase  $\text{TiO}_2$  nanocrystal film as ECL without any further treatments (Scheme 1). Finally, the utilization of this new approach was strongly indicated by efficient inverted OSCs.

## Experimental section

### Materials

$\text{TiCl}_3$  (15.0–20.0% basis in 30% HCl) and tetrabutyl titanate were purchased from Aladdin. Other chemicals used for synthesis were purchased from Beijing Chemical Works. P3HT and PCBM were purchased from Rieke Metals and Nano-C respectively and used as received. 1,2-dichlorobenzene was purchased from Sigma-Aldrich and used without further purification.

### Synthesis of $\text{TiO}_2$ nanocrystals

The anatase  $\text{TiO}_2$  nanocrystals were synthesized in a facile and moderate procedure: the mixture of  $\text{TiCl}_3$  (15%–20%, 2 mL) and HCl (6 mol/L, 2 mL) in ethanol (30 mL) was heated at 90 °C for 6 h in an autoclave, followed by aging at room temperature for one week without further treatment. Before use, the  $\text{TiO}_2$  nanoparticle dispersion was filtered through a 0.8  $\mu\text{m}$  nylon syringe filter.

### Preparation of nanocrystal $\text{TiO}_2$ film

The  $\text{TiO}_2$  layer was obtained by spin-coating the dispersion of  $\text{TiO}_2$  nanocrystals in ethanol at 2000 rpm for 1 min on ITO substrate and dried in air for 1 hour. The thickness of this  $\text{TiO}_2$  layer in this spin-coating condition was estimated to be about 25–30 nm from the FE-SEM cross-section images (inset of Fig. 2a) and could be varied systematically by changing the spin-coating parameters or repeating the spin-coating process several times as needed.

### Preparation of annealed $\text{TiO}_2$ film

4 mL tetrabutyl titanate was dissolved in 2 mL isopropanol in a conical flask for 5 min. 210  $\mu\text{L}$  water and 17  $\mu\text{L}$  concentrated HCl were mixed with 4 mL isopropanol for 5 min, then this solution was dropped into the conical flask over about 10 min, and the mixture was stirred for 12 h at room temperature. Before use, the resultant  $\text{TiO}_x$  precursor was diluted with isopropanol in the volume ratio of 1:3. The diluted solution was filtered through a 0.8  $\mu\text{m}$  nylon syringe filter and then spin-coated (4000 rpm for 1 min) on ITO substrate and annealed at 400 °C for 30 min.

### Device fabrication

The ITO glasses ( $\sim 20 \Omega/\text{cm}^2$ ) were ultrasonically cleaned in detergent, deionized water, acetone and isopropyl alcohol. After routine solvent cleaning, the substrates were treated by  $\text{O}_2$  plasma for 10 min. The  $\text{TiO}_2$  layer (nanocrystal  $\text{TiO}_2$  layer or

annealed  $\text{TiO}_2$  layer) was obtained by spin-coating without or with high temperature annealing as discussed before. Following that, an active layer was deposited on top of the  $\text{TiO}_2$  layer by spin-coating a solution of the P3HT and PCBM blend with a weight ratio of 1:1 in 1,2-dichlorobenzene (40 mg/mL) at 700 rpm for 60 s in  $\text{N}_2$  environment. The active layer was then dried in covered glass petri dishes for 1 hour without further thermal annealing. Finally, a  $\text{MoO}_3$  layer (5.5 nm) and an Ag layer (100 nm) were deposited by vacuum thermal evaporation and a metal shadow mask was used to define the device area of 5  $\text{mm}^2$ . The current density–voltage ( $J$ – $V$ ) characteristics of the devices were measured in air using a Keithley 2400 parameter analyzer under a simulated light (AM 1.5G) with intensity of 100  $\text{mW}/\text{cm}^2$ .

### Characterizations

X-Ray diffraction (XRD) study was performed on Bruker AXS D8 Focus apparatus using Cu K $\alpha$  radiation ( $\lambda = 1.54056 \text{ \AA}$ ). Ultraviolet photoelectron spectroscopy (UPS) spectra were recorded using a PREVAC XPS/UPS System under He irradiation ( $h\nu = 21.2 \text{ eV}$ ). The transmittance of the  $\text{TiO}_2$  films (on ITO/glass) was characterized using an UV-3600 Shimadzu UV–vis–NIR Spectrophotometer. Field emission scanning electron microscope (FE-SEM) images were measured on a JEOL JSM 4800F. Transmission electron microscope (TEM) images were taken using an FEI Tecnai G2 operated at 200 kV. The atomic force microscopy (AFM) measurements were performed on an S II Nanonavi probe station 300 HV (Seiko, Japan) in contact mode.

## Results and discussion

$\text{TiO}_2$  nanoparticles were synthesized in a mild and facile procedure without any additional surfactants or binders. The morphologies of the resulted  $\text{TiO}_2$  nanoparticles were characterized by TEM measurement. As shown in Fig. 1a, ultrafine and homogeneous  $\text{TiO}_2$  nanoparticles were obtained by this method and the sizes distributed mainly in the range of 2–3 nm (inset of Fig. 1a), which were quite essential for fabricating high-quality  $\text{TiO}_2$  film by spin-coating (*vide infra*). The crystalline phase of  $\text{TiO}_2$  nanoparticles was determined carefully by HRTEM and XRD measurements. As shown in the inset of Fig. 1b, the apparent lattice fringes ( $d_{200} = 0.19 \text{ nm}$ ) on the particles revealed the anatase crystallization<sup>26</sup> and the assembled nanoparticles on the substrate exhibited continuous crystalline regions (Fig. S1 in ESI<sup>†</sup>), which proved a good crystallinity degree of the nanoparticle assembled film. Meanwhile, the XRD pattern (Fig. 1b) of the  $\text{TiO}_2$  nanocrystal film confirmed that the film was composed of small size anatase nanocrystals due to the widened standard anatase diffraction peaks (JCPDS no. 21-1272). It should be noted that the anatase  $\text{TiO}_2$  nanocrystals prepared by this method were dispersed well in ethanol to form transparent colloid solution without any additional surfactants or binders which were undesired for fabricating high-quality  $\text{TiO}_2$  layer because they would bring organic impurities and needed thermal decomposition to remove. This character combining with the

advantage of ultrafine sizes of the  $\text{TiO}_2$  nanoparticles enabled us to fabricate a transparent and compact  $\text{TiO}_2$  layer by simply spin-coating the nanocrystal dispersion. It should be highlighted that the  $\text{TiO}_2$  layer produced by this method was already pre-crystallized to anatase phase and able to directly apply as ECL in thin film photovoltaics without further crystallization treatments involving of annealing step. In order to study the advantages of room-temperature processed nanocrystal  $\text{TiO}_2$  layer as ECL in depth, conventional  $\text{TiO}_2$  layer which was deposited from  $\text{TiO}_x$  sol-gel and then annealed at  $400^\circ\text{C}$  to obtain anatase phase was prepared on ITO substrate for comparison.

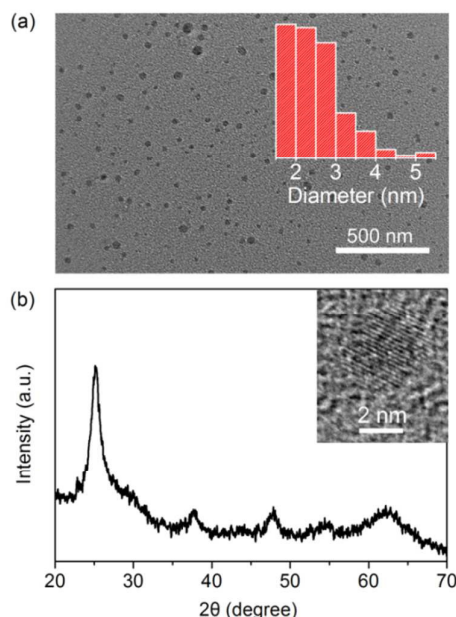


Fig. 1 (a) TEM image of the  $\text{TiO}_2$  nanoparticles. Inset shows the size distribution histogram (155 particles measured), (b) XRD pattern of the anatase  $\text{TiO}_2$  nanocrystals. Inset is HRTEM crystalline lattice fringes.

The morphology of the spin-coated anatase  $\text{TiO}_2$  nanocrystal film was studied by FE-SEM and AFM measurements. In the FE-SEM images (Fig. 2a), tiny nanocrystals assembled tightly to form compact layer. Because of the ultrafine size of the nanocrystals, interspaces between neighbouring particles could be drastically avoided to consolidate the film and benefit the electrical contact to electron transport. Both the top view and cross-section FE-SEM images (Fig. 2a) showed that the nanocrystal  $\text{TiO}_2$  film was compact with no visible cracks or porosity, providing the important foundation for this film to serve as ECL. There were partial raised clusters on the nanocrystalline film surface and the AFM measurement revealed that the root mean square (RMS) surface roughness of the film was 5.77 nm (Fig. 2b), which is obviously higher than that of the conventional high-temperature annealed  $\text{TiO}_2$  film (0.98 nm, Fig. S2 in ESI<sup>†</sup>). The higher roughness derived from the nanoparticle assembled surface could enhance the  $\text{TiO}_2$ /active layer interfacial surface area, which might be benefit to the carrier collection at the

interface of ECL and active layer with shorter electron-hole diffusion lengths comparing with the film thickness.<sup>27-29</sup>

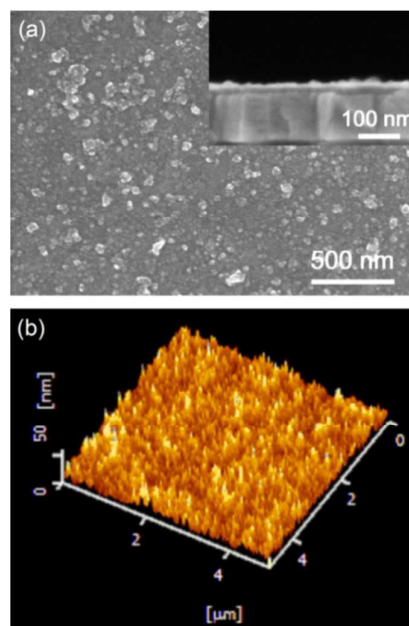


Fig. 2 (a) Top view and cross-section (inset) FE-SEM images of the  $\text{TiO}_2$  nanocrystal film. (b) AFM image of the  $\text{TiO}_2$  nanocrystal film.

The optical transmittance spectra of various  $\text{TiO}_2$  films on ITO substrates, including nanocrystalline  $\text{TiO}_2$ /ITO prepared by this method, conventional high-temperature annealed  $\text{TiO}_2$ /ITO and bare ITO, were compared (Fig. 3), and the thickness of the  $\text{TiO}_2$  films on ITO was consistent with that in the optimized OSCs. Compared with bare ITO, the  $\text{TiO}_2$  nanocrystal film could decrease the transmittance of ultraviolet light (350–400 nm) and enhance the transmittance beyond 450 nm. The decrease of transmittance in the ultraviolet region was caused by the absorption of the nanocrystal  $\text{TiO}_2$  film (Fig S3 in ESI<sup>†</sup>). This feature could protect the active layer from UV radiation and simultaneously enhance the transmittance of incident light in visible region. The protection effect of  $\text{TiO}_2$  film to active layer by decreasing the transmittance of ultraviolet (350–400 nm) light was investigated through time-dependent absorption measurements under the irradiation of simulated AM 1.5 sunlight. The active layers on the ITO/PEDOT:PSS substrate and ITO/ $\text{TiO}_2$  substrate were irradiated under AM 1.5 sunlight, and the absorption spectra were recorded at various time. As shown in Fig S4 of ESI<sup>†</sup>, the absorbances are decreased gradually along with extending irradiation time. After irradiation of 7 h, 98.86% and 98.00% of initial absorbances are remained for the active layers on the substrates with and without  $\text{TiO}_2$  layer, respectively. It directly proves the protection effect of  $\text{TiO}_2$  film to active layer by decreasing the transmittance of ultraviolet light. For the annealed  $\text{TiO}_2$ /ITO, the transmittance decreased on a large scale especially in range of 420–580 nm, probably due to the destruction of ITO film during the high-temperature treatment.<sup>19</sup> In most high-



temperature processed  $\text{TiO}_2$  based solar cells, thermostable substrate such as FTO was explored instead of ITO, which would bring with low transmittance and conductivity for the electrode. Herein, the utilization of the room-temperature processed nanocrystal  $\text{TiO}_2$  layer not only protected ITO from thermal destruction but also enabled the fabrication of solar cells on other thermal sensitive substrates such as polyethyleneterephthalate (PET).<sup>2</sup>

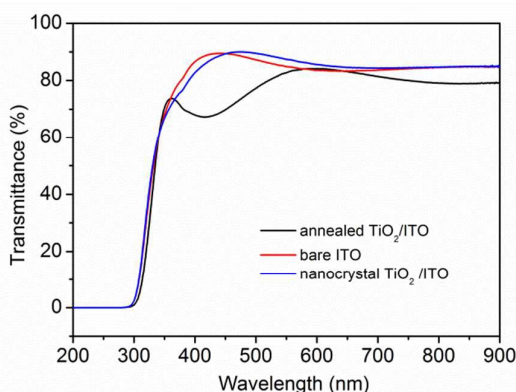


Fig. 3 Optical transmittance spectra of nanocrystal and annealed  $\text{TiO}_2$  films on ITO substrates.

The electronic properties, in terms of energy levels and electron mobility, of the  $\text{TiO}_2$  nanocrystal film were also studied. Based on the UPS and UV-Vis absorption spectra (Fig. S5 and S6 in ESI<sup>†</sup>), the valence band (VB) and band gap of the  $\text{TiO}_2$  nanocrystal film were determined to be 7.0 eV and 3.3 eV respectively, and as a consequence, the conduction band (CB) was calculated to be 3.7 eV. The energy levels of this  $\text{TiO}_2$  nanocrystal film were in good agreement with those of other reported  $\text{TiO}_2$  ECLs,<sup>18, 19</sup> which demonstrated its energy-aligning capability as effective ECL. The electron mobility of the  $\text{TiO}_2$  nanocrystal film was estimated by the space charge limited current (SCLC) method (Fig. S7 in ESI<sup>†</sup>) and the value of  $2.7 \times 10^{-3} \text{ cm}^2 \text{ V}^{-1} \text{ s}^{-1}$  could surpass that of the previously reported anatase  $\text{TiO}_2$  nanorods ( $2.33 \times 10^{-4} \text{ cm}^2 \text{ V}^{-1} \text{ s}^{-1}$ ) measured by the same method.<sup>30</sup> These electronic properties endow the  $\text{TiO}_2$  nanocrystal film with effective electron collecting and transporting ability.

In order to illustrate the utilization of the  $\text{TiO}_2$  nanocrystal film with favourable morphology, optical and electronic properties, a prove-of-concept inverted OSC has been fabricated which explored the  $\text{TiO}_2$  nanocrystal film as ECL (device 1). On the pre-clean ITO substrate, the  $\text{TiO}_2$  nanocrystal film was fabricated by spin-coating the dispersion of  $\text{TiO}_2$  nanocrystals in ethanol. Without any further treatment on the  $\text{TiO}_2$  nanocrystal film, a P3HT:PCBM active layer, a  $\text{MoO}_3$  layer and an Ag electrode were deposited successively (for details, please see experiment section). Fig. 4a showed a FE-SEM cross-section of the device and illustrated the schematic device structure. Device 1 exhibited a satisfying photovoltaic performance with an open circuit voltage ( $V_{oc}$ ) of 0.59 V, a short-circuit current density ( $J_{sc}$ ) of  $9.27 \text{ mA cm}^{-2}$ , a fill

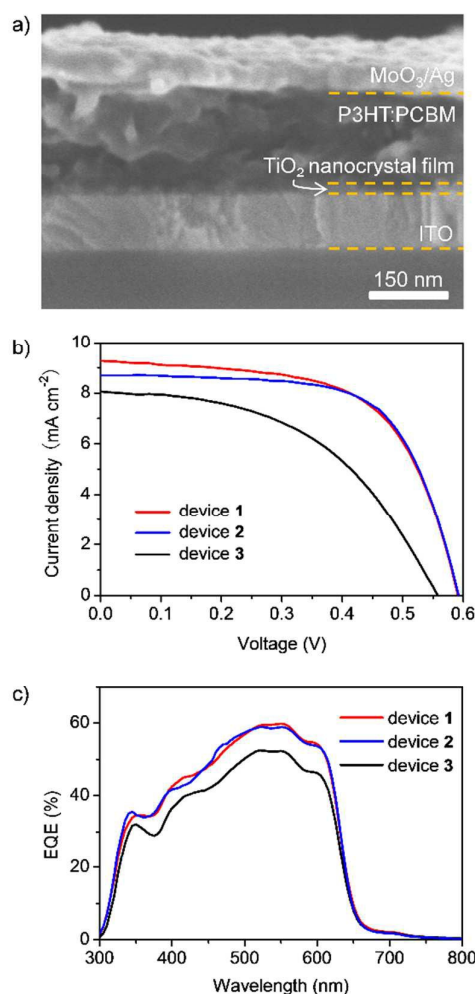


Fig. 4 (a) FE-SEM cross-section image of device 1. (b) Current density versus voltage ( $J$ - $V$ ) curves of device 1–3 (with the structures of device 1: ITO/ $\text{TiO}_2$  nanocrystal layer (25–30 nm)/P3HT:PCBM (210 nm)/ $\text{MoO}_3$  (5.5 nm)/Ag (70 nm), device 2: ITO/PEDOT:PSS (40 nm)/P3HT:PCBM (210 nm)/LiF (1 nm)/Al (100 nm), and device 3: ITO/annealed  $\text{TiO}_2$  layer (35 nm)/P3HT:PCBM (210 nm)/ $\text{MoO}_3$  (5.5 nm)/Ag (70 nm)). (c) EQE spectra of devices 1–3.

factor (FF) of 0.61, and an overall power conversion efficiency (PCE) of 3.35% (best value of 30 devices with an average PCE of 3.11%) respectively under simulated AM 1.5 ( $100 \text{ mW cm}^{-2}$ ) sunlight (Fig. 4b). The performance of device 1 was comparable to that of the conventional OSC (device 2 with the structure of ITO/PEDOT:PSS (40 nm)/P3HT:PCBM (210 nm)/LiF (1 nm)/Al (100 nm)) with high-performance PCE of 3.39%. (Fig. 4b) This result strongly illustrated the effective electron collection and transport abilities of the nanocrystal  $\text{TiO}_2$  layer and the feasibility to explore the  $\text{TiO}_2$  nanocrystal film as ECL for OSCs. In addition, a reference inverted OSC (device 3) with traditionally high-temperature annealed  $\text{TiO}_2$  as ECL was fabricated on ITO substrate for comparison. The performance of device 3 gave a reduction on  $V_{oc}$ ,  $J_{sc}$ , FF and thus an overall PCE which are 0.56 V,  $8.07 \text{ mA cm}^{-2}$ , 0.48 and 2.18% respectively (Fig. 4b), due to the optical and electronic

alteration of ITO/TiO<sub>2</sub> layers under high-temperature annealing.<sup>19, 31</sup> This comparison highlighted the advantage of fabricating TiO<sub>2</sub> nanocrystal film using this method in moderate condition to avoid the undesired high-temperature treatment on TiO<sub>2</sub> ECL.

To gain a deep insight into the effect of TiO<sub>2</sub> nanocrystal film, the external quantum efficiency spectrum (EQE) of device **1** was measured and compared with that of devices **2-3**. As shown in Fig 4c, the EQE spectrum of device **1** with TiO<sub>2</sub> nanocrystal film is comparable with that of conventional device **2**. The maximum of EQE value is 60% at 555 nm for device **1**. In contrast, the EQE spectrum of device **3** with high-temperature annealed TiO<sub>2</sub> film is much lower, and the maximum of EQE value decreases to 52% at 520 nm. The EQE measurements further indicate the effectiveness and advantage of the TiO<sub>2</sub> nanocrystal film fabricated by this annealing-free method.

## Conclusion

An extremely convenient and moderate approach to fabricate anatase TiO<sub>2</sub> nanocrystal film as electron collection layer in photovoltaics has been developed. Ultrafine, clean and high-quality anatase TiO<sub>2</sub> nanocrystal dispersion has been prepared in a simple route and spin-coating the nanocrystal dispersion at room temperature provides a well performed TiO<sub>2</sub> nanocrystal layer. It should be noted that, without any further treatments (such as high temperature annealing), the TiO<sub>2</sub> nanocrystal film exhibited favourable morphology, optical and electronic properties, and in consequence was successfully applied as ECL in inverted OSC. This approach has overcome the ugly defect of high-temperature annealing process in traditional fabrication of anatase TiO<sub>2</sub> ECLs. As thin TiO<sub>2</sub> ECLs are broadly used in other thin film solar cells such as inverted hybrid solar cells and planar perovskite solar cells besides OSCs, the annealing-free TiO<sub>2</sub> nanocrystal film has the potential to be employed in other photovoltaic systems and will meet further demands for low temperature processing plastic solar cells.

## Acknowledgements

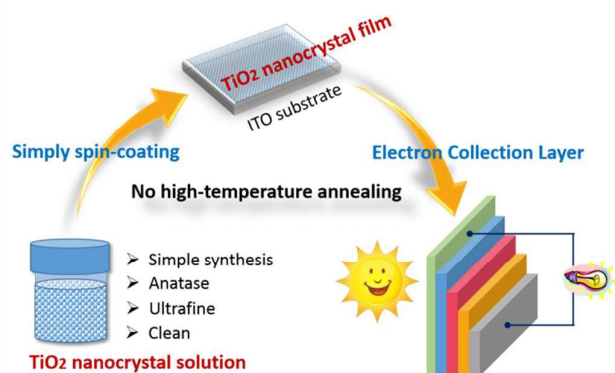
This work was supported by the National Natural Science Foundation of China (61306081, 61176016), Natural Science Foundation of Jilin Province (20130522142JH, 20121801).

## Notes and references

- G. Yu, J. Gao, J. C. Hummelen, F. Wudl and A. J. Heeger, *Science*, 1995, **270**, 1789-1791.
- F. C. Krebs, *Sol. Energy Mater. Sol. Cells*, 2009, **93**, 394-412.
- S. H. Park, A. Roy, S. Beaupre, S. Cho, N. Coates, J. S. Moon, D. Moses, M. Leclerc, K. Lee and A. J. Heeger, *Nat. Photonics*, 2009, **3**, 297-302.
- F. C. Krebs, N. Espinosa, M. Hösel, R. R. Søndergaard and M. Jørgensen, *Adv. Mater.*, 2014, **26**, 29-39.
- L. Lu, T. Zheng, Q. Wu, A. M. Schneider, D. Zhao, L. Yu, *Chem. Rev.*, 2015, DOI: 10.1021/acs.chemrev.5b00098.

- R. Steim, F. R. Kogler and C. J. Brabec, *J. Mater. Chem.*, 2010, **20**, 2499-2512.
- F.-x. Xie, W. C. H. Choy, W. E. I. Sha, D. Zhang, S. Zhang, X. Li, C.-w. Leung and J. Hou, *Energy Environ. Sci.*, 2013, **6**, 3372-3379.
- M. Graetzel, R. A. J. Janssen, D. B. Mitzi and E. H. Sargent, *Nature*, 2012, **488**, 304-312.
- C.-Y. Li, T.-C. Wen, T.-H. Lee, T.-F. Guo, J.-C.-A. Huang, Y.-C. Lin and Y.-J. Hsu, *J. Mater. Chem.*, 2009, **19**, 1643-1647.
- E. J. W. Crossland, N. Noel, V. Sivaram, T. Leijtens, J. A. Alexander-Webber and H. J. Snaith, *Nature*, 2013, **495**, 215-219.
- K. Lee, J. Y. Kim, S. H. Park, S. H. Kim, S. Cho and A. J. Heeger, *Adv. Mater.*, 2007, **19**, 2445-2449.
- H. Sun, J. Weickert, H. C. Hesse and L. Schmidt-Mende, *Sol. Energy Mater. Sol. Cells*, 2011, **95**, 3450-3454.
- A. Hagfeldt and M. Grätzel, *Acc. Chem. Res.*, 2000, **33**, 269-277.
- A. Karpinski, S. Berson, H. Terrisse, M. Mancini-Le Granvalet, S. Guillerez, L. Brohan and M. Richard-Plouet, *Sol. Energy Mater. Sol. Cells*, 2013, **116**, 27-33.
- H. Hänsel, H. Zettl, G. Krausch, R. Kisselev, M. Thelakkat and H. W. Schmidt, *Adv. Mater.*, 2003, **15**, 2056-2060.
- M. Liu, M. B. Johnston and H. J. Snaith, *Nature*, 2013, **501**, 395-398.
- J. T.-W. Wang, J. M. Ball, E. M. Barea, A. Abate, J. A. Alexander-Webber, J. Huang, M. Saliba, I. Mora-Sero, J. Bisquert, H. J. Snaith and R. J. Nicholas, *Nano Lett.*, 2014, **14**, 724-730.
- K.-L. Ou, D. Tadytin, K. Xerxes Steirer, D. Placencia, M. Nguyen, P. Lee and N. R. Armstrong, *J. Mater. Chem. A*, 2013, **1**, 6794-6803.
- J.-H. Huang, H.-Y. Wei, K.-C. Huang, C.-L. Chen, R.-R. Wang, F.-C. Chen, K.-C. Ho and C.-W. Chu, *Energy Environ. Sci.*, 2010, **3**, 654-658.
- Z. Lin, C. Jiang, C. Zhu and J. Zhang, *ACS Appl. Mater. Interfaces*, 2013, **5**, 713-718.
- H. C. Weerasinghe, P. M. Sirimanne, G. V. Franks, G. P. Simon and Y. B. Cheng, *J. Photochem. Photobiol. A: Chem.*, 2010, **213**, 30-36.
- H. Lee, D. Hwang, S. M. Jo, D. Kim, Y. Seo and D. Y. Kim, *ACS Appl. Mater. Interfaces*, 2012, **4**, 3308-3315.
- D. Liu and T. L. Kelly, *Nat. Photonics*, 2014, **8**, 133-138.
- K. Wojciechowski, M. Saliba, T. Leijtens, A. Abate and H. J. Snaith, *Energy Environ. Sci.*, 2014, **7**, 1142-1147.
- B. Conings, L. Baeten, T. Jacobs, R. Dera, J. D'Haen, J. Manca, and H.-G. Boyen, *APL Mater.*, 2014, **2**, 081505.
- H. G. Yang, G. Liu, S. Z. Qiao, C. H. Sun, Y. G. Jin, S. C. Smith, J. Zou, H. M. Cheng and G. Q. Lu, *J. Am. Chem. Soc.*, 2009, **131**, 4078-4083.
- W.-H. Baek, I. Seo, T.-S. Yoon, H. H. Lee, C. M. Yun and Y.-S. Kim, *Sol. Energy Mater. Sol. Cells*, 2009, **93**, 1587-1591.
- F. J. Lim, A. Krishnamoorthy and G. W. Ho, *ACS Appl. Mater. Interfaces*, 2015, **7**, 12119-12127.
- Q. Z. Orawan Wiranwetchayan, Xiaoyuan Zhou, and P. S. Zhiqiang Liang, Guozhong Cao, *Chalcogenide Lett.*, 2012, **9**, 157-163.
- Y.-C. Tu, J.-F. Lin, W.-C. Lin, C.-P. Liu, J.-J. Shyue and W.-F. Su, *CrystEngComm*, 2012, **14**, 4772-4776.
- Ref: The high temperature annealing process leads to a serious degree of In species diffusion between the TiO<sub>2</sub> and ITO films, which lowers the conductivity of ITO and bring quenching centers into TiO<sub>2</sub> layer, thus has a negative effect on the efficiency.

## TOC Figure



Annealing-free TiO<sub>2</sub> electron collection layer in organic solar cell based on ultrafine, clean and high-quality anatase TiO<sub>2</sub> nanocrystals.